A prion-like domain in ELF3 functions as a thermosensor in Arabidopsis

Jae-Hoon Jung, Antonio Barbosa, Stephanie Hutin, Janet Kumita, Mingjun Gao, Dorothee Derwort, Catarina Silva, Xuelei Lai, Elodie Pierre, Feng Geng, et al.

A prion-like domain in ELF3 functions as a thermosensor in Arabidopsis

Authors:

Jae-Hoon Jung[1,2]*, Antonio D. Barbosa[1]*, Stephanie Hutin[4]*, Janet R. Kumita[3], Mingjun Gao[1], Dorothee Derwort[1], Catarina S. Silva[4], Xuelei Lai[1,4], Elodie Pierre[4], Feng Geng[1], Sol-Bi Kim[2], Sujeong Baek[2], Chloe Zubieta[4], Katja E. Jaeger[1,5] and Philip A. Wigge[1,5,6]

[1]Sainsbury Laboratory, University of Cambridge, Cambridge, CB2 1LR, United Kingdom.
[2]Department of Biological Sciences, Sungkyunkwan University, Suwon 16419, South Korea.
[3]Department of Chemistry, University of Cambridge, Lensfield Rd, Cambridge CB2 1EW, United Kingdom.
[4]Laboratoire de Physiologie Cellulaire and Végétale, Université Grenoble Alpes/CNRS/CEA/INRAE, 17 Rue des Martyrs, 38054 Grenoble, France.
[5]Leibniz-Institut für Gemüse- und Zierpflanzenbau, Theodor-Echtermeyer-Weg 1, 14979 Großbeeren, Germany.
[6]Institute of Biochemistry and Biology, University of Potsdam, 14476 Potsdam, Germany.

*These authors contributed equally
§Corresponding author: wigge@igzev.de

----------(Introductory paragraph, 271 words) ----------

Temperature is a major environmental variable governing plant growth and development, and climate change has already altered the phenology of wild-plants and crops[1]. However, the mechanisms by which plants sense temperature are not well understood. Environmental signals, including temperature, are integrated into growth and developmental pathways via the circadian clock and the activity of the Evening Complex (EC), a major signalling hub and core clock component[2,3]. The EC acts as a temperature responsive transcriptional repressor, providing rhythmicity and temperature responsiveness to growth via unknown mechanisms[2,4–6]. The EC consists of EARLY FLOWERING3 (ELF3)[4,7], a large scaffold protein and key component

in temperature sensing, ELF4, a small alpha helical protein, and LUX ARRYTHMO (LUX), a DNA binding protein required for recruitment of the EC to transcriptional targets. ELF3 contains a polyglutamine (polyQ) repeat[8–10], embedded within a predicted prion domain (PrD). We find the length of the polyQ repeat correlates with thermal responsiveness. ELF3 in plants from hotter climates, which have no detectable PrD domain, is active at high temperature and these plants lack thermal responsiveness. ELF3 temperature sensitivity is also modulated by the levels of ELF4, indicating that ELF4 can stabilise ELF3 function. In both Arabidopsis and a heterologous system, ELF3-GFP forms speckles within minutes in response to higher temperatures in a PrD-dependent manner. This suggests that ELF3 is thermosensory. A purified fragment encompassing the ELF3 PrD reversibly forms liquid droplets in response to temperature *in vitro,* indicating that these properties reflect a direct biophysical response conferred by the PrD. The ability of temperature to rapidly convert ELF3 between active and inactive states via phase transition represents a novel thermosensory mechanism.

----------(Main text, 1605 words) ----------

Arabidopsis ELF3 contains a polyglutamine (polyQ) repeat which varies from 7 to 29 residues in length in natural populations, and has been associated with phenotypic variation[8–10] (Fig. 1a). We therefore investigated if the length of the polyQ repeat influences ELF3 activity. We find that in an isogenic Col-0 background, complementing *elf3-1* with *ELF3* transgenes encoding increasing polyQ lengths results in increased sensitivity to warm temperature as measured by hypocotyl elongation (Fig. 1b, Extended Data Fig. 1, Extended Data Fig. 14). The effects of altering polyQ length are mild, in agreement with other studies[8,11], and Q0 lines are still thermally responsive. This indicated that additional features of ELF3 are also required for responding to temperature. Since the polyQ repeat is located in the centre of a region predicted to be a prion domain[12] (PrD; residues 430-609) (Fig. 1a), we hypothesized that this might confer temperature responsiveness. If the PrD of ELF3 plays a role in temperature responsiveness in Arabidopsis, we wondered if it varies in plants adapted to different climates. Indeed, ELF3 from *Solanum tuberosum* and *Brachypodium distachyon* are not predicted to have

PrD regions (Fig. 1a; Extended Data Fig. 2). Since accelerated flowering is a major adaptive response of Arabidopsis to warm temperature, we investigated if *StELF3* and *BdELF3* alter this trait. *BdELF3* and *StELF3* are functional in Arabidopsis and complement *elf3-1* (Extended Data Fig. 3). At 22 ºC these plants resemble wild-type, however at 27 ºC they lose almost all their thermally responsive early flowering (Fig. 1c). This shows that these versions of ELF3 lacking a PrD are largely unable to respond to warm temperature. To test whether the thermal responsiveness of Arabidopsis ELF3 is due to the PrD itself, we created a chimeric version, where we replaced the PrD of Arabidopsis with the corresponding sequence of BdELF3 (Extended Data Fig. 2). Chimeric ELF3-BdPrD shows a suppression of temperature responsive flowering, confirming that the PrD from Arabidopsis confers thermal responsiveness (Fig. 1c).

The activity of ELF3 is modulated by binding to the small peptide ELF4[13]. To further understand if ELF4 is contributing to the thermal responsiveness of ELF3, we investigated the effect of temperature on hypocotyl elongation and flowering time in *elf4-101* and *elf4-2*. At 22 and 27 ºC, *elf4* alleles largely resemble *elf3-1*, consistent with the key role for ELF4 in the EC[2,13]. At 17 ºC, *ELF4* becomes dispensable for controlling both hypocotyl elongation and flowering time and *elf4-101* and *elf4-2* have similar phenotypes to Col-0 (Fig. 2a). These results suggest that ELF4 plays a role in buffering the temperature responsiveness of ELF3 at higher temperatures, leading us to hypothesize that overexpressing *ELF4* may stabilize ELF3, as is suggested by *in vitro* studies[15]. *ELF4* expression is circadianly regulated, peaking at the end of the day and rapidly declining during the night[14]. We observe that plants constitutively overexpressing *ELF4* are largely unable to respond to temperature, as seen by both hypocotyl elongation and flowering time (Fig. 2b), indicating that the presence of higher levels of ELF4 is sufficient to maintain ELF3 in the active state even at 27 ºC (Fig. 2b). This appears to be a consequence of modulating ELF3 function, since overexpressing *ELF4* has no detectable effect in the *elf3-1* background, and *ELF3* overexpression does not change thermal responsiveness (Extended Data Fig. 4). We mapped the

domain of ELF3 that interacts with ELF4 to a low complexity region adjacent to the PrD (Extended Data Fig. 11).

Since ELF3 is a temperature dependent transcriptional repressor, we sought to determine if the phenotypic variation in responsiveness to temperature can be accounted for by variation in occupancy of ELF3 on target genes. As shown previously[3,4], the occupancy of ELF3 on target genes decreases with warmer temperature (Fig. 2c, Extended Data Fig. 5). Consistent with our phenotypic observations, forms of ELF3 lacking a PrD also lose their temperature responsiveness of binding, indicating that the PrD directly modulates the thermoresponsiveness of ELF3 binding at target genes (Fig. 2d, Extended Data Fig. 4). Finally, overexpressing *ELF4* is also sufficient to stabilize ELF3 binding and abolish the temperature response (Fig. 2e, Extended Data Fig. 5).

Since ELF3 functions as a transcriptional regulator we sought to determine if our observed changes in occupancy have a detectable influence on the *ELF3*-dependent transcriptome. To identify *ELF3*-dependent genes, we searched for genes showing a pattern of expression similar to *LUX*, i.e. having a strong up-regulation in *elf3-1* and a reduced expression in *ELF3-OE* at ZT8 and ZT12. In this way we were able to identify 325 genes whose expression is dependent on the level of *ELF3* activity, which includes key EC targets such as *PIF4* and *GI*. These genes are less thermally responsive in backgrounds expressing *BdELF3* or overexpressing *ELF4* (Extended Data Fig. 6, 7 and 8). We observe a mild effect of the polyQ lines on the expression of *ELF3*-dependent genes, consistent with the more subtle phenotypes for hypocotyl length we observe for these lines (Extended Data Fig. 6, 7). We find 112 genes associated with the strongest ELF3 ChIP-seq peaks, and 25 of these are common with the 325 *ELF3*-dependent genes, consistent with this being a direct mechanism (Extended Data Fig. 8). The *ELF3*-dependent genes directly bound by ELF3 show a clear temperature responsiveness in their expression, and this is affected when ELF3 binding is stabilized.

To investigate if temperature may directly control ELF3 activity, we analyzed the behaviour of natively expressed ELF3-GFP *in planta*. At 17 ºC, ELF3-GFP is nuclear with a diffuse signal. Upon shifting to 35 ºC, we see multiple bright speckles form, a behaviour that is specific to the presence of the PrD, since the chimeric ELF3 with the BdPrD remains largely diffuse in response to warmer temperature (Fig. 3a). This behaviour is also observed at 27 ºC (Fig. 3b). Increasing polyQ length also results in a greater tendency to form speckles (Extended Data Fig. 9). Since ELF3 *in planta* may be influenced by other factors that have co-evolved to control its activity, we sought to determine if ELF3 expressed in *Saccharomyces cerevisiae*, a heterologous system lacking *ELF3* related genes, is temperature responsive. Under a low expression system, ELF3-GFP forms a largely diffuse signal in yeast cells, while when highly expressed, it forms bright puncta or speckles (Fig. 3c). We next investigated the influence of temperature on ELF3-GFP in yeast. At 19 ºC, the signal is largely diffuse. Shifting cells to 35 ºC results in a rapid formation of sharp punctate GFP signals, that is more significant for ELF3 Q7 and Q35 compared to ELF3 BdPrD or free GFP (Fig. 3d, e). These effects appear specific for ELF3, since 35 ºC is below the temperature required for endogenous proteins to aggregate[16], and we observe robust cell growth and protein expression under these conditions (Extended Data. Fig. 10). While classically prions are associated with stable insoluble aggregates in the cell, the EC and ELF3 undergo diurnal cycles of activity and temperatures fluctuate over short timescales, suggesting reversibility of the temperature response is likely important. Indeed, the EC rapidly returns to full activity when plants are shifted from 27 to 22 ºC[4], leading us to hypothesize that the formation of speckles may be reversible. This is the case in yeast, as returning cells from 35 to 19 ºC results in a rapid reduction in the number of speckles (Fig. 3f, g).

The results so far are consistent with ELF3 being able to adopt two conformations: an active soluble form, and, at higher temperatures, a higher order multimeric form that is visible as bright speckles. It has been suggested that a major biological function of prion-like proteins is to act as environmental switches, as they are able to rapidly change conformation and form liquid droplets[17]. While ELF3 is largely insoluble *in vitro*, we identified a soluble

peptide fragment spanning the PrD (ELF3 PrD, residues 388-625). AtELF3 PrD, in contrast to BdELF3 PrD, rapidly and reversibly forms liquid droplets as a function of ionic strength, protein concentration and temperature (Fig. 4a, b, Extended Data 12). To analyze the dynamics of this behaviour, we purified ELF3 PrD fused to GFP (PrD-GFP). Decreasing the salt concentration and pH induces PrD-GFP to undergo a phase transition, forming micron sized spherical droplets. The droplets are highly mobile in solution and are able to fuse, indicative of phase separated liquids (Fig. 4c and Extended Data Fig. 13a, b). Using fluorescence recovery after photobleaching (FRAP) we see that recovery fractions range from 0.1 to 0.8 with recovery half-lives from seconds to minutes (Fig. 4d and Extended Data Fig. 13c, d). To determine if the PrD is thermoresponsive, we analyzed liquid droplet formation as a function of temperature. The purified ELF3 PrD peptide is more soluble at low temperature, but undergoes a sharp phase transition with a midpoint at 28.7 ±1.8 ºC under our conditions (Fig. 4e). Upon decreasing the temperature, this process is significantly reversible and the cycle can be repeated (Fig. 4f). This agrees with the temperature responsiveness of the ELF3 system in *Arabidopsis* seedlings, where the strongest phenotypic effects are observed at 27 ºC. This response is specific for the PrD, since the equivalent peptide fragment of BdELF3 shows no liquid droplet formation (Fig. 4e). These results indicate that the PrD domain of ELF3 serves as a tunable thermosensor. Intrinsically disordered proteins frequently display thermoresponsive liquid-liquid phase separation, a behaviour driven by solvent-mediated interactions in a sequence dependent manner[18]. Since PrD and intrinsically disordered protein sequences are widespread within eukaryotes[19], it will be interesting to see if they have been recruited to provide thermosensory behaviour via phase transitions in other signalling contexts, such as the reversible aggregation of proteins in response to heat stress in yeast[16].

----------(End of main text)----------

We thank M. Perutz for discussions on polyQ proteins. We thank the microscopy facility MuLife of IRIG/DBSCI, funded by CEA Nanobio and labex Gral for equipment access and use and Laëtitia Kurzawa and Fabrice Senger for technical assistance and helpful discussions. This work used the platforms

of the Grenoble Instruct-ERIC Center (ISBG : UMS 3518 CNRS-CEA-UGA-EMBL) with support from FRISBI (ANR-10-INBS-05-02) and Labex GRAL (ANR-CBH-EUR-GS) within the Grenoble Partnership for Structural Biology (PSB). PW and CZ received funding from Instruct-ERIC (PID: 2236). This work has supported by the National Research Foundation of Korea(NRF) grant funded by the Korea government(MSIT)(No. 2019R1C1C1010507 to J.-H.J). This work was funded by ANR-19-CE20-0021-01 PRC (CZ). PAW receives funding from the Leibniz Foundation.

Data Availability Statement:

Sequencing data for gene expression analysis (RNA-seq) and protein-DNA interactions (ChIP-seq) have been deposited in the publicly available databasej GEO, Accession Code GSE137264, with review access token "mjqdmmamvtsdret".

Code Availability:
The code to produce the figures from the processed files is available at https://github.com/shouldsee/polyq-figures . To enable easier browsing, a static site is hosted at https://shouldsee.github.io/polyq-figures . The inhouse pipeline for mapping is available at https://github.com/shouldsee/synoBio .

Author contributions:
JHJ, ADB, SH, JRK, CZ, KEJ and PAW conceived the study and wrote the manuscript. JHJ, MG generated transgenic plants and mutants and analysed their phenotypes. ADB performed in vivo imaging experiments in yeasts and plants. SH, JRK, CSS, XL, EP, CZ performed and analysed in vitro phase separation assays. KEJ performed ChIP- and RNA-seq experiments. DD and FG analysed sequencing data. SBK and SB performed yeast two hybrid assays and analysed gene expression levels in transgenic plants. CZ, KEJ and PAW supervised experimental work.

References:

1. Scheffers, B. R. *et al.* The broad footprint of climate change from genes to biomes to people. *Science (80-.).* **354**, aaf7671 (2016).
2. Nusinow, D. A. *et al.* The ELF4-ELF3-LUX complex links the circadian clock to diurnal control of hypocotyl growth. *Nature* **475**, 398–402 (2011).
3. Ezer, D. *et al.* The evening complex coordinates environmental and endogenous signals in Arabidopsis. *Nat. Plants* **3**, 17087 (2017).
4. Box, M. S. *et al.* ELF3 controls thermoresponsive growth in Arabidopsis.

Curr. Biol. **25**, 194–9 (2015).

5. Mizuno, T. *et al.* Ambient Temperature Signal Feeds into the Circadian Clock Transcriptional Circuitry Through the EC Night-Time Repressor in Arabidopsis thaliana. *Plant Cell Physiol.* **0**, 1–19 (2014).
6. Raschke, A. *et al.* Natural variants of ELF3 affect thermomorphogenesis by transcriptionally modulating PIF4-dependent auxin response genes. *BMC Plant Biol.* **15**, 197 (2015).
7. Nieto, C., Lopez-Salmeron, V., Daviere, J. & Prat, S. ELF3-PIF4 interaction regulates plant growth independently of the Evening Complex. *Curr. Biol.* **25**, 187–193 (2015).
8. Undurraga, S. F. *et al.* Background-dependent effects of polyglutamine variation in the Arabidopsis thaliana gene ELF3. *Proc. Natl. Acad. Sci. U. S. A.* **109**, 19363–7 (2012).
9. Tajima, T., Oda, A., Nakagawa, M., Kamada, H. & Mizoguchi, T. Natural variation of polyglutamine repeats of a circadian clock gene ELF3 in Arabidopsis. *Plant Biotechnol* **24**, 237–240 (2007).
10. Jiménez-Gómez, J. M., Wallace, A. D. & Maloof, J. N. Network analysis identifies ELF3 as a QTL for the shade avoidance response in arabidopsis. *PLoS Genet.* **6**, (2010).
11. Press, M. O. & Queitsch, C. Variability in a short tandem repeat mediates complex epistatic interactions in Arabidopsis thaliana. *Genetics* (2017). doi:10.1534/genetics.116.193359
12. Lancaster, A. K., Nutter-Upham, A., Lindquist, S. & King, O. D. PLAAC: a web and command-line application to identify proteins with prion-like amino acid composition. *Bioinformatics* **30**, 2501–2502 (2014).
13. Herrero, E. *et al.* EARLY FLOWERING4 recruitment of EARLY FLOWERING3 in the nucleus sustains the Arabidopsis circadian clock. *Plant Cell* **24**, 428–43 (2012).
14. Doyle, M. R. *et al.* The ELF4 gene controls circadian rhythms and flowering time in Arabidopsis thaliana. *Nature* **419**, 74–77 (2002).
15. Silva, C. S. *et al.* Molecular mechanisms of Evening Complex activity in Arabidopsis. *Proc. Natl. Acad. Sci.* **XX**, XX (2020).
16. Wallace, E. W. J. *et al.* Reversible, Specific, Active Aggregates of Endogenous Proteins Assemble upon Heat Stress. *Cell* (2015).

doi:10.1016/j.cell.2015.08.041
17. Franzmann, T. M. *et al.* Phase separation of a yeast prion protein promotes cellular fitness. *Science* **359**, eaao5654 (2018).
18. Dignon, G. L., Zheng, W., Kim, Y. C. & Mittal, J. Temperature-Controlled Liquid–Liquid Phase Separation of Disordered Proteins. *ACS Cent. Sci.* acscentsci.9b00102 (2019). doi:10.1021/acscentsci.9b00102
19. Si, K. Prions: What Are They Good For? *Annu. Rev. Cell Dev. Biol.* **31**, 149–169 (2015).

FIGURE LEGENDS

Fig. 1: The polyQ repeat of ELF3 is embedded within a predicted prion-domain which is essential for thermal responsiveness.

a, Arabidopsis ELF3 (AtELF3) contains a polyQ repeat embedded with a predicted prion-domain (PrD), while this PrD signature is absent in ELF3 from *Brachypodium distachyon* (BdELF3) and *Solanum tuberosum* (SdELF3). Prion domains predicted using PLAAC[12]. **b**, At 17 ºC, *ELF3* is required to prevent hypocotyl elongation, but different polyQ lengths in ELF3 do not perturb ELF3 function. At 27 ºC, the responsiveness of ELF3 to temperature increases with the length of the polyQ. (Naming convention: Q7-17, 7 refers to length of polyQ repeat, and 17 is the individual transgenic line used in the study). **c,** The ELF3 PrD plays a critical role in the thermal control of flowering time. Overexpressing AtELF3 does not change the thermal induction of flowering, indicating that simply increasing ELF3 protein level is not sufficient to delay flowering, while overexpressing BdELF3 causes an almost complete loss of thermal induction, and StELF3 has a milder influence. These effects are also apparent when BdELF3 is expressed using the native ELF3 promoter, and dependent on the PrD, since replacing this domain of AtELF3 with the corresponding Bd sequence is sufficient to greatly reduce the thermal induction of flowering.

Fig. 2: *ELF4* is required to stabilize the activity of the EC at warmer temperatures.

a, At lower temperatures, *ELF4* becomes dispensable for controlling both hypocotyl elongation and flowering, but with increasing temperature, *ELF4*

assumes a greater role. **b**, *ELF4* overexpression reduces thermal responsiveness of hypocotyl elongation and markedly decreases the flowering time response to temperature, and this response is entirely dependent on *ELF3*. **c**, ELF3 binding at targets, which is measured by ChIP-seq, is temperature dependent and declines genome-wide at 27 ºC. **d**, Transgenic plants with stabilized forms of ELF3 do not respond to temperature. **e**, *ELF4* overexpression stabilizes ELF3 and removes its temperature responsiveness of binding to targets. Scale bars, 5 mm (**a**, **b**)

Fig. 3: High temperature induces the formation of reversible ELF3 speckles *in vivo*.

a, Seedlings expressing GFP-tagged ELF3 (Q7) or a chimeric ELF3 where the PrD has been replaced by the corresponding region of Brachypodium ELF3 (BdPrD) grown in short photoperiods for 7 days at 17 ºC. Roots imaged by confocal microscopy before and after incubation at 35 ºC for 15 min. **b**, Seedlings as in (a) but shifted to 27 ºC for 2 h. c, *S. cerevisiae cells* expressing GFP-tagged ELF3 (Q7) from a centromeric plasmid (Low) or an episomal plasmid (High), to achieve low or high expression levels of the protein, were grown in selective synthetic complete medium at 30 ºC; Sec63-mCherry was used as an ER reporter. **d**, Quantification of ELF3 speckles in S. cerevisiae cells expressing free GFP (GFP only), ELF3 (Q7), ELF3 with a longer polyQ repeat (Q35), or ELF3 with the PrD of B. distachyon (BdPrD) grown overnight at 19 ºC and incubated at the indicated temperatures for 30 min. **e**, representative images of cells from d at 35 ºC . **f**, S. cerevisiae cells expressing ELF3 were grown at 19 ºC overnight and incubated at 35 ºC for 30 min (19 > 35) followed by incubation at 19 ºC for 60 min (35 > 19). **g**, Quantification of ELF3 speckles for cells in f. Scale bars, 40 μm (a and b) and 5 μm (a and b inset, c, e, and f) , ** $p < 0.01$.

Fig. 4: The PrD of ELF3 undergoes a reversible phase transition in response to temperature.

a, Purified ELF3 PrD peptide forms liquid droplets at 27 ºC *in vitro.* **b**, The equivalent protein domain from BdELF3, which is not predicted to contain a

PrD, remains soluble and does not show any liquid droplet formation **c**, Purified ELF3 PrD-GFP protein forms spherical droplets *in vitro*, which fuse. **d**, ELF3 PrD-GFP droplets show rapid recovery after photobleaching, indicating they are liquid droplets. **e**, Light scattering assay as a function of temperature for ELF3 PrD (15 μM; black circle), BdELF3 (15 μM; grey circle) and buffer alone (50 mM CAPS pH 9.7, 150 mM NaCl, 1 mM TCEP; open triangles). Dashed line shows curve-fitting using a 4-parameter sigmoidal equation. The T_m for ELF3 PrD is 28.7 ± 1.8 ºC and the spectrum is representative of three independent experiments. **f**, Reversibility of light scattering as a function of temperature for ELF3 PrD (15 μM; 50 mM CAPS pH 9.7, 200 mM NaCl, 1 mM TCEP). On the same sample, the temperature was increased and decreased three times in succession (1 °C/min). The observed turbidity was reversible and consistently returned to Abs_{440nm} = 0.432 ± 0.02. Interestingly, the initial absorbance reading for repeat 3 (Ab_{440nm} = 0.288) is lower than for repeat 2 (Abs_{440nm} = 0.373) and this is likely due to time dependent equilibration (as noted in Extended Figure 12**c**). .The spectra are representative of two independent experiments and similar results were observed for samples at 5 μM. Scale bars, 50 μm (**a**, **b**) and 5 μm (**c**, **d**).

EXTENDED DATA FIGURE LEGENDS

Extended Data Fig. 1 | The length of the polyQ repeat within the ELF3 PrD influences temperature responsiveness.

Hypocotyl length of transgenic plants with altered polyQ lengths at different temperatures. Data for 17 and 27 ºC are used in **Fig. 1b**.

Extended Data Fig. 2 | Multiple sequence alignment of ELF3 proteins generated with ClustalW. ELF3 amino acid sequences from three different plant species were included in the alignment. The region indicated by an arrow were used to create a chimeric version of *Arabidopsis* ELF3, where the ELF3 PrD was replaced with the corresponding sequence of BdELF3 or StELF3.

Extended Data Fig. 3 | Plants expressing ELF3 lacking a detectable PrD from potato (St) and Brachypodium (Bd) rescue *elf3-1* at 22 ºC and show reduced *FT* expression.

A, and **b**. Transgenic plants in the *elf3-1* background expressing different forms of *ELF3* expressed constitutively (*35S* promoter) or under the endogenous *AtELF3* promoter ($ELF3_{pro}$) grown in SD conditions until bolting. **c**, Relative expression of *FT* at zeitgeber time (ZT) 8 was analyzed by RT-qPCR. Twelve-day-old seedlings grown at different temperatures under short photoperiod conditions (SDs) were used to analyze transcript accumulation. Bars indicate standard error of the mean.

Extended Data Fig. 4 | ELF4 modulates the temperature responsiveness of EC activity.

At low temperatures, *ELF4* is dispensable, and *elf4-2* mutants have similar hypocotyl phenotypes to wild-type plants. As temperature increases, the role of *ELF4* becomes increasingly important, as measured by hypocotyl length. Overexpressing *ELF3* (*ELF3-OE*) is not sufficient to change thermal responsiveness and *ELF3* overexpression has no effect in the *elf4-2* background at 27 ºC, indicating that *ELF4* plays an important role at higher temperatures.

Extended Data Fig. 5 | The binding of ELF3 at target genes depends on temperature, and stabilized forms of ELF3 are less temperature responsive than wild-type ELF3.

Average ELF3 ChIP-seq peak signals are measured as fold-enrichment over input (as calculated by MACS2) across multiple transgenic lines expressing different ELF3 variants.

Extended Data Fig. 6 | The expression of *ELF3* dependent genes is influenced by temperature and the PrD of ELF3.

325 transcripts having *ELF3* dependent expression were analyzed in RNA-seq datasets for different genotypes at 22 and 27 ºC. As expected, gene expression is generally suppressed at 22 ºC (red), apart from in the case of the *elf3-1* background, where genes are up-regulated (green). Lines

overexpressing *BdELF3* show less activation at 27 ºC, consistent with their later flowering phenotypes. Just replacing the *Arabidopsis* PrD with the corresponding region from BdELF3 (in the *ELF3pro::BdELF3* at 27 ºC) is sufficient to greatly reduce the upregulation of *ELF*3 dependent genes at 27 ºC. Up-regulation of *ELF3* dependent genes also occurs in an *elf3-1* mutant when *ELF4* is overexpressed, consistent with *ELF3* being necessary for *ELF4* action.

Extended Data Fig. 7 | The expression of *ELF3* dependent genes is influenced by temperature and the polyQ repeat of ELF3.
325 transcripts having *ELF3* dependent expression were used analyzed in RNA-seq datasets for different genotypes at 22 and 27 ºC. Plants expressing ELF3 with a truncated polyQ repeat (ELF3-Q0) show a reduced expression of *ELF3* dependent genes at 27 ºC, consistent with their shorter hypocotyl phenotype.

Extended Data Fig. 8 | *ELF3* target genes show altered responsiveness to temperature in backgrounds where stabilized versions of ELF3 are expressed.
Heat map showing that ELF3 bound targets that are usually induced by shifting to 27 ºC (green) become less temperature responsive in backgrounds where ELF3 is more stable.

Extended Data Fig. 9 | The length of the polyQ repeat within the ELF3 PrD influences speckle formation by temperature *in vivo*.
a, Arabidopsis seedlings expressing GFP-tagged ELF3 variants with either no polyQ repeat (Q0), the WT polyQ (Q7), a polyQ with 20 or 30 glutamines (Q20 and Q30, respectively), or the PrD replaced by the corresponding region from *Brachypodium distachyon* ELF3 (BdPrD). Seedlings were grown in short photoperiods for 7 days at 17 ºC. Roots were imaged by confocal microscopy before and after incubation at 30 ºC for 15 min. **b**, Quantification of the degree of speckle formation in (a). Regions of the roots corresponding to the size of individual cells were selected, and the mean, standard deviation (sd) and maximum (max) gray value were measured in ImageJ. It was assumed that

speckle formation would lead to higher gray values and higher frequency of speckles within the analysis region would increase the standard deviation. **c**, Relative *FT* expression in the *ELF3pro::ELF3-GFP* transgenic plants examined. Relative expression of *FT* at zeitgeber time (ZT) 8 was analyzed by RT-qPCR. Twelve-day-old seedlings grown at different temperatures under SDs were used to analyze transcript accumulation. Bars indicate standard error of the mean. Warm temperature effect on the induction of *FT* was not observed only in the transgenic plants containing ELF3 variants with the BdPrD. Scale bar, 40 μm (**a**).

Extended Data Fig. 10 | Yeast strains show no growth defect after incubation at the indicated temperatures used in the speckle formation experiments and express detectable levels of ELF3-GFP

a, Temperature shifts do not affect yeast viability. Yeast cells were grown overnight at 19°C and shifted to the indicated temperatures for 30 min (as done in temperature shifts used for speckle inductions). Serial dilutions were spotted onto YPD plates and incubated at 30°C for the indicated times. **b**, Yeast cells expressing the indicated ELF3-GFP constructs or an empty vector were grown overnight in selective media to exponential phase at 30°C. Cells (approximately 9 OD600) were pelleted, washed with sterile water, and lysed in 100 μl SDS-sample buffer with 0.5 mm diameter glass beads (BioSpec Products, Bartlesville, OK) by two rounds of boiling for 2 min and vortexing for 30 sec. Protein extracts were centrifuged at 13,000 rpm for 15 min, and the supernatants analysed by Western blot using anti-GFP antibody (a gift from A. Peden). Western blot signals were developed using ECL (GE Healthcare, Little Chalfont UK).

Extended Data Fig. 11 | ELF3-ELF4 protein-protein interactions in yeast cells

a, ELF3 constructs used. Numbers indicate reside positions. PrD, prion-related domain. The domain structure of the ELF3 protein was determined using SMART protein domain annotation resource (http://smart.embl.de). ELF3 does not contain any specific domains except for low complexity regions, which are regions in protein sequences that differ from the

composition and complexity of most proteins with normal globular structure. **b**, Interactions of ELF3 with ELF4 in yeast cells. Cell growth on selective media was examined. Please note that the ELF3 region containing a low complexity region, which is not overlapped with PrD sequence, is responsible for the interaction with ELF4. A soluble form of ELF3 peptide, which is used for *in vitro* experiments, does not include the region required for the interaction with ELF4.

Extended Data Fig. 12 | ELF3 PrD proteins show phase change characteristics *in vitro*.

a, SDS gel (12 % polyacrylamide) for ELF3 peptides for BdELF3 PrD, ELF3 PrD, and ELF3 PrD-GFP. M, molecular weight marker. Proteins were expressed and purified at least ten times with highly reproducible results. **b**, Phase diagram of ELF3 PrD peptide with respect to salt and protein concentration. Examples of phases are shown in the right panel. **c**, Droplet formation is dynamic with droplets re-entering the soluble phase over time as measured from two independent samples (mean shown) by changes in A_{340} after droplet formation induced by dilution from a high salt to low salt buffer (50 mM CAPS, pH 9.7, 1 mM TCEP, 500 to 150 mM NaCl).

Extended Data Fig. 13 | ELF3 PrD droplets fuse.

a, Fusion of two droplets over time with intensity profiles of each droplet shown below the images. **b**, Fusion of ELF3 PrD droplets. Two examples are shown. **c**, Example of photobleaching and recovery over time. Images were taken (left to right) before, after and at time points 30 s, 120 s, 240 s post-photobleaching. **d**, FRAP recovery curves for **c** and mean +/- SD. Droplet fusions and FRAP experiments were performed over five times with reproducible results.

Extended Data Fig. 14 | *ELF3* expression in the transgenic lines used in this study

Please note that all transgenic plants used in this study were generated by expressing *ELF3* gene under the control of its native promoter in the *elf3-1*

mutant backgrounds. Phenotypes of the *elf3-1* mutant were perfectly rescued in all *ELF3* transgenic lines used in this study. Transcript levels of *ELF3* gene were determined by RT-qPCR. Gene expression values were normalized to the *eIF4A* expression. Biological triplicates were averaged. Error bars indicate standard error of the mean. **a**, *ELF3pro::ELF3 elf3-1* transgenic plants without any tag sequences. They were used for hypocotyl elongation and RNA-seq experiments. **b**, *ELF3pro::ELF3-FLAG elf3-1* lines were used for flowering time measurements and ChIP-seq experiments . **c**, *ELF3pro::ELF3-GFP elf3-1* lines were used for observation of ELF3 speckle formation *in planta*.

METHODS ONLINE

Generation of transgenic plants used in study

Arabidopsis thaliana lines used in this study were in Columbia (Col-0) background. The *elf3-1, elf4-2*, and *elf4-101* mutants have been described previously[2–4]. To generate transgenic plants overexpressing *ELF4* gene (*ELF4-OE*), the *ELF4* coding sequence was subcloned into pENTR-D-TOPO vector (ThermoFisher Scientific, Rockford, IL) according to the manufacturer's procedure. The resultant entry plasmid was recombined with LR clonase into the gateway binary pJHA212B vector containing the 35S promoter and C-terminal 3xflag tag sequences. The binary construct was transformed into Col-0 plants by floral dipping method. The *ELF4-OE* transgenic plants were isolated by basta selection, and propagated to obtain single insertion lines with phenotypes of short hypocotyls and delayed flowering. The *ELF3-OE* transgenic plant has been described previously[4]. The *ELF3-OE* and *ELF4-OE* plants were crossed with *elf4-2* and *elf3-1*, respectively and the resultant homozygous generations were used for measurements of hypocotyl length and flowering time.

To investigate if the length of the polyglutamine (polyQ) repeat influences ELF3 activity, a 7.8 kb genomic fragment of *ELF3* including its promoter and stop codon was firstly subcloned into pENTR-D-TOPO vector, as described above. Please note that the ELF3 protein in Col-0 plant has the

polyQ repeat sequence of Q7. The Q7 repeat sequence in the entry plasmid was deleted or extended to Q21 by an overlapping PCR strategy. Three kinds of entry plasmids encoding ELF3 proteins with Q0, Q7, and Q21, respectively, were was recombined with LR clonase into the gateway binary pJHA212K vector without any tagging sequences. The binary construct was transformed into the *elf3-1* mutant by floral dipping method. Three kinds of transgenic plants were isolated by kanamycin selection and propagated to obtain single insertion lines rescuing the long hypocotyl phenotype in the *elf3-1*. The resultant homozygous generations were used for hypocotyl length measurements.

To investigate if the prion domain (PrD) in the ELF3 protein confers thermal responsiveness, we generated transgenic plants expressing *StELF3* and *BdELF3* under the control of both the native *Arabidopsis ELF3* and 35S promoters in *elf3-1*. Genomic DNA was first isolated from the nuclei of *Solanum tuberosum* and *Brachypodium distachyon* using a standard CTAB DNA extraction method. Coding sequences of *StELF3* and *BdELF3* genes were amplified by PCR using the genomic DNA from *Solanum* and *Brachypodium*, respectively, as template. The PCR fragments were cloned into the SLIC binary vector containing the 35S promoter and N-terminal 3xflag tag sequences using NEBuilder® HiFi DNA Assembly Cloning Kit (New England BioLabs, Hertfordshire, UK), and the constructs were transformed into the *elf3-1* mutant, resulting in *StELF3-OE* and *BdELF3-OE*, respectively. The same PCR fragments were also cloned into the SLIC binary vector containing the *Arabidopsis ELF3* promoter and C-terminal 3xflag tag sequences, and the constructs were transformed into the *elf3-1* mutant, resulting in *ELF3pro:StELF3* and *ELF3pro:BdELF3* transgenic plants, respectively. To create a chimeric version of *Arabidopsis* ELF3, where its PrD was replaced with the corresponding sequence of BdELF3, the existing entry plasmid containing the *Arabidopsis ELF3* promoter and coding region was modified to replace the DNA fragment encoding PrD sequence (residues 430-609aa) with the corresponding DNA fragment of *BdELF3* gene (Expended Data Fig. 2). The modified entry plasmid was recombined with LR clonase into the gateway binary pJHA212K vector containing the C-terminal 3xflag tag sequence, and the constructs were transformed into the *elf3-1* mutant,

resulting in the *ELF3pro:ELF3-BdPrD* transgenic plant. All transgenic plants containing DNA fragments from *Solanum* or *Brachypodium* were isolated by kanamycin selection and propagated to obtain single insertion lines rescuing the long hypocotyl phenotype in the *elf3-1*.

Different kinds of ELF3 entry plasmids encoding *Arabidopsis* ELF3 proteins with the variation of polyQ length (Q0~Q35) or *Brachypodium* ELF3 protein were recombined into the gateway binary pJHA212K vectors containing the C-terminal 3xflag or GFP tag sequences. The resultant constructs were transformed into the *elf3-1* mutant for generating transgenic plants used for chromatin immunoprecipitation sequencing (ChIP-seq) or plant fluorescence microscopy experiments, respectively. The *ELF3pro*:*ELF3-MYC elf3-1* transgenic plant used for ChIP-seq experiments has been described previously[3].

Plant growth conditions

Arabidopsis seeds were sterilized and sown on standard half-strength Murashige and Skoog-agar (MS-agar) plates at pH 5.7. Sterilized seeds were stratified for 3 days at 4 ºC in the dark and allowed to germinate for 24 hours at 22 ºC under cool-white fluorescent light at 170 μmol m^{-2} s^{-1}. The plates were then transferred to short photoperiod conditions (SDs, 8-h light and 16-h dark) at different temperatures for assays. For hypocotyl length measurement, 7- or 8-day-old seedlings, which were grown under SDs with light intensity of 80 μmol m^{-2} s^{-1}, were photographed and analyzed using ImageJ software (http://rsbweb.nih.gov/ij/).

For flowering time measurement, plants were grown in soil under SDs at either 22 or 27 ºC until flowering. Flowering times were determined by counting the number of rosette and cauline leaves at bolting. Twenty to thirty plants were counted and averaged for each measurement.

ChIP-seq experiments

Seedlings were grown for 10 days under SDs at either 17 or 22 ºC and shifted to 27 ºC for 2 h at ZT8. 3 g of seedlings for each treatment were fixed under vacuum for 20 min in 1xPBS (10 mM PO_4^{3-}, 137 mM NaCl, and 2.7 mM KCl) containing 1% Formaldehyde (F8775 Sigma). The reaction was quenched by

adding glycine to a final concentration of 62 mM. ChIP experiments were performed as described[20]. Anti-c-Myc agarose affinity gel antibody (Sigma, A7470), Anti-HA−Agarose (Sigma, A2095) or Anti-Flag® M2 Affinity Gel (Sigma, A2220) were used for immunoprecipitation. Sequencing libraries were prepared using TruSeq ChIP Sample Preparation Kit (Illumina, IP-202-1024) or using NEBNext® Ultra™ II DNA Library Prep Kit (New England BioLabs) and samples were sequenced on the Illumina NextSeq 500 platform.

RNA-seq experiments

Seedlings were grown on plates for 10 days and harvested at the indicated time points. 70 mg of seedlings were pooled per tube and total RNA was extracted using MagMAX™-96 Total RNA Isolation Kit (ThermoFisher) according to the manufacturer‘s instruction. Libraries were prepared using Lexogen QuantSeq 3' mRNA-Seq Library Prep FWD Kit (Illumina) according to manufacturer‘s instruction. The libraries were sequenced on the Illumina NextSeq 500 platform.

Bioinformatic analysis of ChIP-seq and RNA-seq data

Pipeline: Quantification of gene expression and chipseq binding:
Figure: pile-up figure: Coverage values were extracted from RPKM bigwig outputs from the pipeline for [File:"chipseq_differential_binding.peak_list.csv"]. The figure is shaded with standard error computed for each x-value.
File: "chipseq_differential_binding.peak_list.csv"

Two ELF3 ChIP-Seq libraries were compared to shortlist 362 1bp genomic intervals that show reduced binding in 27C compared to 17C. These genomic intervals are used for pileup of other ChIP-Seq libraries.

File: "chipseq_targets_genes_job.peak_list.csv"

Continuing from "chipseq_differential_binding.peak_list.csv", the genomic intervals are filtered out if it lacks an annotated start codon within 500bp. These genes are then deposited into

File: "chipseq_differential_binding.peak_list.csv"

Column:"chipseq_targets_genes_job"

see "chipseq_targets_genes_job.peak_list.csv"

Column: "signature_targets"

A signature_score is computed for each of ~36k annotated genes, according to their similarity to a signature gene LUX within 10 selected datasets. The top 1% genes were then selected to be "signature_targets". The signature score is defined as

s=<meanNorm(expression(gene)),meanNorm(expression(LUX))>s=<meanNorm(expression(gene)),meanNorm(expression(LUX))>

where <expr1,expr2><expr1,expr2> is the dot product taken over the selected datasets.

Analysis of gene transcript levels

Gene transcript levels were determined by RT-qPCR. Isolation of total RNA from appropriate plant materials was carried out using Trizol reagent (Thermo Fisher Scientific) according to the manufacturer's recommendations. First strand cDNA was synthesized from 1.5 µg of total RNA using RevertAid First Strand cDNA Synthesis Kit (Thermo Fisher Scientific) according to the manufacturer's recommendations. RT-qPCR reactions were performed in 96-well blocks with the QuantStudio 1 Real-Time PCR System (Thermo Fisher Scientific) using the TOPreal qPCR 2XPreMIX (SYBR Green with high ROX, Enzynomics, Daejeon, Korea) in a final volume of 20 µl. The PCR primers used are listed in Table. The values for each set of primers were normalized relative to the EUKARYOTIC TRANSLATION INITIATION FACTOR 4A1 (eIF4A) gene (At3g13920). All RT-qPCR reactions were performed in three technical replicates using total RNA samples extracted from three independent biological replicate samples.

Gene	**Forward primer**	**Reverse primer**
ELF3	TCTAGTCAGCCTTGTGGTGTG	TCCTCTGATCATGCTGTGCC

FT	GGTGGAGAAGACCTCAGGAA	GGTTGCTAGGACTTGGAACATC
eIF4A	TGACCACACAGTCTCTGCAA	ACCAGGGAGACTTGTTGGAC

Plant fluorescence microscopy

Seeds were sown on MS-agar plates and stratified for two to three days at 4 ºC in the dark. The plates were then transferred into short photoperiod conditions and grown for 7 days at 17 ºC. Roots were imaged before and after incubation of the slides at 35 ºC for 15 min, or after 2 hours of incubation of the seedlings on pre-warmed MS-agar plates at 27 degrees, on a Zeiss LSM880 upright confocal microscope with a 20× dry Plan-Apochromatic 0.8 NA objective lens and acquired using ZEN 2.3 software (Carl Zeiss Ltd, Jena, Germany). GFP fluorescence was excited with a 488 nm line from an argon laser. Images were saved as czi files and then subsequently imported to ImageJ software.

For calculating the speckle score based on flurorescence intensity (Extended Data Fig. 9), regions of the roots corresponding to the size of individual cells were selected, and the mean, standard deviation (sd) and maximum (max) gray value were measured in ImageJ. It was assumed that speckle formation would lead to higher gray values and higher frequency of speckles within the analysis region would increase the standard deviation. A speckle score was obtained by calculating the ratio of the max gray value and the mean gray value, normalised to the average of the mean gray values for all the regions measured in each root (to account for local intensity variation), and finally multiplied by the standard deviation, according the following formula:

speckle score = [max(grey value)/mean(grey value)]/average(mean grey value for all regions in the root) x sd

Yeast fluorescence microscopy

Yeast cells (RS453 *MATα ade2-1 his3-11,15 ura3-52 leu2-3112 trp1-1, URA3::YIplac211-SEC63-mCherry*)[21] were transformed with plasmids in the table below using the lithium acetate method, and grown in synthetic defined (SD) medium containing 0.17% Yeast Nitrogen Base (MP Biomedicals, Santa

Ana, CA), 0.5% ammonium sulfate (Fisher Scientific, Leicestershire, UK), -LEU/-TRP DO supplement (Clontech, Kusatsu, Japan), and 60 mg l^{-1} leucine or 40 mg l^{-1} tryptophan (Sigma, St. Louis, MO), for plasmid selection. Cells were grown overnight at 19 ºC, incubated at 35 ºC for 30 min and, where indicated, re-incubated at 19 ºC for 60 min. Cells were imaged live in a Zeiss AxioImager.Z2 epifluorescence upright microscope with a 100× Plan-Apochromatic 1.4 NA objective lens (Carl Zeiss Ltd, Jena, Germany). Images were recorded using a large chip sCMOS mono camera for sensitive fluorescence imaging (ORCA Flash 4.0v2, Hamamatsu, Hamamatsu, Japan), saved by Zeiss ZEN2.3 software (Blue edition, Carl Zeiss Ltd, Jena, Germany) and exported to ImageJ software.

Plasmid	Description	Source
YCplac111-NOP-GFP	GFP under the control of *NOP1* promoter in *LEU2/CEN* vector	S. Siniossoglou Lab
YCplac111-NOP-cELF3-Q7-GFP	C-terminally GFP tagged WT ELF3 cDNA under the control of *NOP1* promoter in *LEU2/CEN* vector	This study
YCplac111-NOP-cELF3-Q35-GFP	C-terminally GFP tagged ELF3 cDNA with a polyQ repeat containing 35 glutamines under the control of *NOP1* promoter in *LEU2/CEN* vector	This study
YCplac111-NOP-cELF3-BdPrD-GFP	C-terminally GFP tagged ELF3 cDNA with the PrD domain of *B. distachyon* under the control of *NOP1* promoter in *LEU2/CEN* vector	This study
pGBKT7-cELF3-Q7-GFP	C-terminally GFP tagged WT ELF3 cDNA under the control of *ADH1* promoter in *TRP1/2* vector	This study

Yeast two hybrid assays

Yeast two-hybrid assays were performed using the BD Matchmaker system (Clontech, Palo Alto, CA). The pGADT7 vector was used for GAL4 activation domain, and the pGBKT7 vector was used for GAL4 DNA-binding domain. Clontech's Y2H Gold yeast strain was used for transformation. ELF4 and ELF3 cDNA sequences were subcloned into pGBKT7 and pGADT7 vectors, respectively. Transformation of vector constructs into Y2H Gold cells was

performed according to the manufacturer's instructions. Colonies obtained were streaked on selective medium without Leu, Trp, His, and Ade (-LWHA).

ELF3 PrD constructs

Arabidopsis ELF3 PrD (residues 388-625, AT2G25930) and *Brachypodium* ELF3 PrD (residues 432-669, BRADI_2g14290) were cloned into the expression vector pESPRIT2[22,23] using the Aat II and Not I sites. The plasmid contains an N-terminal 6-His tag followed by a TEV protease cleavage site. All proteins were overproduced in *E. coli* BL21 Rosetta 2 (Novagen).

Protein Expression and purification

BdELF3 PrD, AtELF3 PrD and AtELF3 PrD-GFP were expressed in *Escherichia coli* BL21, which were induced with 1 mM IPTG (isopropyl-β-d-thiogalactopyranoside), at 18°C overnight. Bacterial pellets were resuspended in resuspension buffer (100 mM CAPS pH 9.7, 300 mM NaCl, 30 mM Imidazole, 1 mM TCEP (tris(2-carboxyethyl)phosphine, Sigma) plus cOmplete protease inhibitor cocktail (Roche). Cells were lysed by sonication and the lysates were centrifuged at 50,000 × g for 30 min at 4°C. For AtELF3 PrD and AtELF3 PrD-GFP, the supernatants were applied to a Ni-NTA column. The bound proteins were washed with 20 CV of resuspension buffer and then with 20 CV of a high salt buffer (100 mM CAPS pH 9.7, 1 M NaCl, 30 mM imidazole and 1 mM TCEP) and eluted with 5 CV of elution buffer (100 mM CAPS pH 9.7, 300 mM NaCl, 300 mM imidazole and 1 mM TCEP). The fractions of interest were pooled and dialyzed overnight at 4 ºC in 50 mM CAPS pH 9.7, 400 mM NaCl and 1 mM TCEP.
For BdELF3 PrD, the pellet was solubilised in 8 M urea, 100 mM CAPS pH 9.7 and 300 mM NaCl. A second centrifugation was performed and the supernatant was applied to a Ni-NTA column pre-equilibrated with equilibration buffer (8 M urea, 100 mM CAPS pH 9.7, 300 mM NaCl, 30 mM imidazole and 1 mM TCEP). The bound protein was washed with 20 CV of equilibration buffer and then with 20 CV high salt buffer for on-column refolding. The protein was eluted with 5 CV of elution buffer. Fractions of interest were pooled and dialyzed overnight at 4 °C in 50 mM CAPS pH 9.7,

300 mM NaCl and 1 mM TCEP. Protein purity was determined via SDS-PAGE.

Liquid droplet formation

To form liquid droplets, the NaCl concentration of the dialysis buffer (50 mM CAPS pH 9.7, 400 mM NaCl and 1 mM TCEP) was gradually decreased using a step gradient at 4 ºC. Droplets were visualized after dialysis. Images were acquired at the 20X objective (LUCPLFLN20xPH1/0.45) on an epifluorescence inverted microscope (CKX41 model) equipped with a pE-300 Cool-LED camera.

AtELF3PrD-GFP FRAP

For droplet visualization and photobleaching experiments of AtELF3PrD-GFP protein, liquid droplet formation was induced by mixing 5 µL of 5 mg/mL AtELF3PrD-GFP with 5 µL 20 mM Tris pH 7.5, 100 mM NaCl, 1 mM TCEP on a glass slide. The drop was covered with a cover slip and quickly mounted onto the EclipseTi-E Nikon inverted microscope as part of the confocal spinning disk system with a CSUX1-A1 Yokogawa confocal head, an Evolve EMCCD camera (Roper Scientific, Princeton Instruments) and a Nikon CFI Plan-APO VC 60x, 1.4 N.A, oil-immersion objective controlled with the MetaMorph (Universal Imaging) software with the autofocus function enabled. For photobleaching experiments, droplets were allowed to adhere to the coverslip prior to photobleaching to minimize droplet movement during the experiment. Acquisition times were approximately 1 s per image. Droplet size was ~2-5 µm with bleaching area of ~ 1 µm for partial bleaching and ~5 µm for full bleaching. Time-lapse images were acquired at 530 nM. Droplet intensity profiles were measured manually for droplet fusion quantification in ImageJ[24]. For FRAP experiments, regions of interest (bleached, unbleached and background) were selected in ImageJ and processed with the easyFRAP webtool[25]. Corrected intensities were fit to a single exponential curve in ImageJ.

Light scattering assay

The light scattering assay was performed in a Cary 100 UV-vis spectrometer (Agilent Technologies UK Ltd., Stockport, UK). The absorbance at 440 nm was monitored for samples containing buffer alone (50 mM CAPS pH 9.7, 150 mM NaCl, 1 mM TCEP), ELF3 PrD (15 µM) or BdELF3 (15 µM) in quartz cuvettes (path length 10 mm) with increasing temperature (4-50 ºC; 1 ºC min^{-1}), and the spectra were normalized with respect to ELF3 PrD. A transition temperature (T_m) was determined by fitting the spectrum with a 4-parameter sigmoidal equation (Sigmaplot 11, Systat Software Inc.). Reported values are an average of three separate experiments. To monitor reversibility, the turbidity was monitored whilst increasing temperature (10 to 40 ºC; 1 ºC min^{-1}) followed by decreasing the temperature (40 to 10 ºC1 ºC min^{-1}) and this cycle was repeated three times in total (ELF3 PrD (5 or 15, µM), 50 mM CAPS pH 9.7, 200 mM NaCl, 1 mM TCEP).

20. Jaeger, K. E., Pullen, N., Lamzin, S., Morris, R. J., & Wigge, P. A. Interlocking feedback loops govern the dynamic behavior of the floral transition in *Arabidopsis*. *Plant Cell* **25**, 820–833 (2013).
21. Barbosa, A. D. et al. Lipid partitioning at the nuclear envelope controls membrane biogenesis. *Mol. Biol. Cell* **26**, 3641–3657 (2015).
22. Guilligay, D. et al. The structural basis for cap binding by influenza virus polymerase subunit PB2. *Nat. Struct. Mol. Biol.* **15**, 500–506 (2008).
23. Tarendeau, F. et al. Structure and nuclear import function of the C-terminal domain of influenza virus polymerase PB2 subunit. *Nat. Struct. Mol. Biol.* **14**, 229–233 (2007).
24. Schindelin, J.; Arganda-Carreras, I. & Frise, E. et al. Fiji: an open-source platform for biological-image analysis. *Nature Methods* **9**, 676-682 (2012).
25. Koulouras G, Panagopoulos A, Rapsomaniki MA, Giakoumakis NN, Taraviras S, Lygerou Z EasyFRAP-web: a web-based tool for the analysis of fluorescence recovery after photobleaching data, *Nucleic Acids Res* 46, W467–W472 (2018).

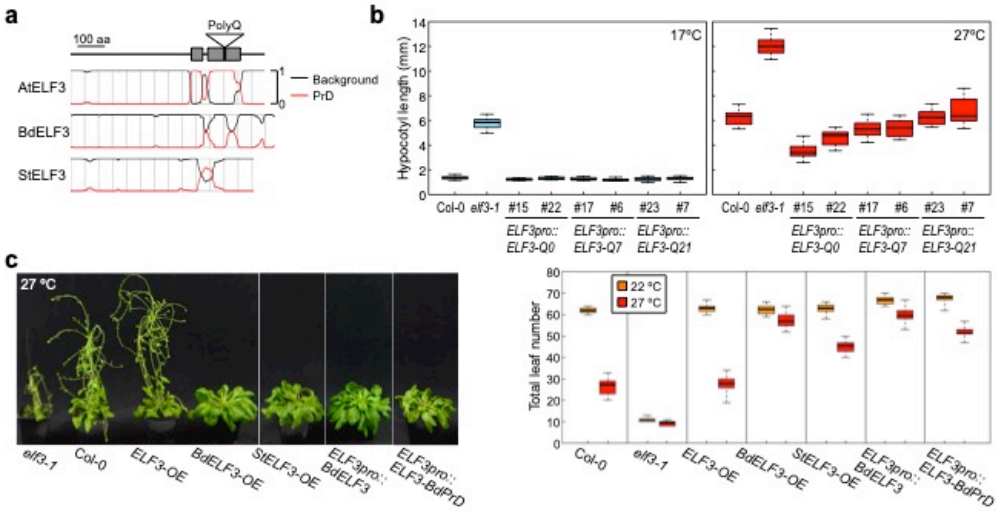

Fig. 1: The polyQ repeat of ELF3 is embedded within a predicted prion-domain which is essential for thermal responsiveness.

a, Arabidopsis ELF3 (AtELF3) contains a polyQ repeat embedded with a predicted prion-domain (PrD), while this PrD signature is absent in ELF3 from *Brachypodium distachyon* (BdELF3) and *Solanum tuberosum* (SdELF3). Prion domains predicted using PLAAC[12]. **b**, At 17 ºC, *ELF3* is required to prevent hypocotyl elongation, but different polyQ lengths in ELF3 do not perturb ELF3 function. At 27 ºC, the responsiveness of ELF3 to temperature increases with the length of the polyQ. (Naming convention: Q7-17, 7 refers to length of polyQ repeat, and 17 is the individual transgenic line used in the study). **c,** The ELF3 PrD plays a critical role in the thermal control of flowering time. Overexpressing AtELF3 does not change the thermal induction of flowering, indicating that simply increasing ELF3 protein level is not sufficient to delay flowering, while overexpressing BdELF3 causes an almost complete loss of thermal induction, and StELF3 has a milder influence. These effects are also apparent when BdELF3 is expressed using the native ELF3 promoter, and dependent on the PrD, since replacing this domain of AtELF3 with the corresponding Bd sequence is sufficient to greatly reduce the thermal induction of flowering.

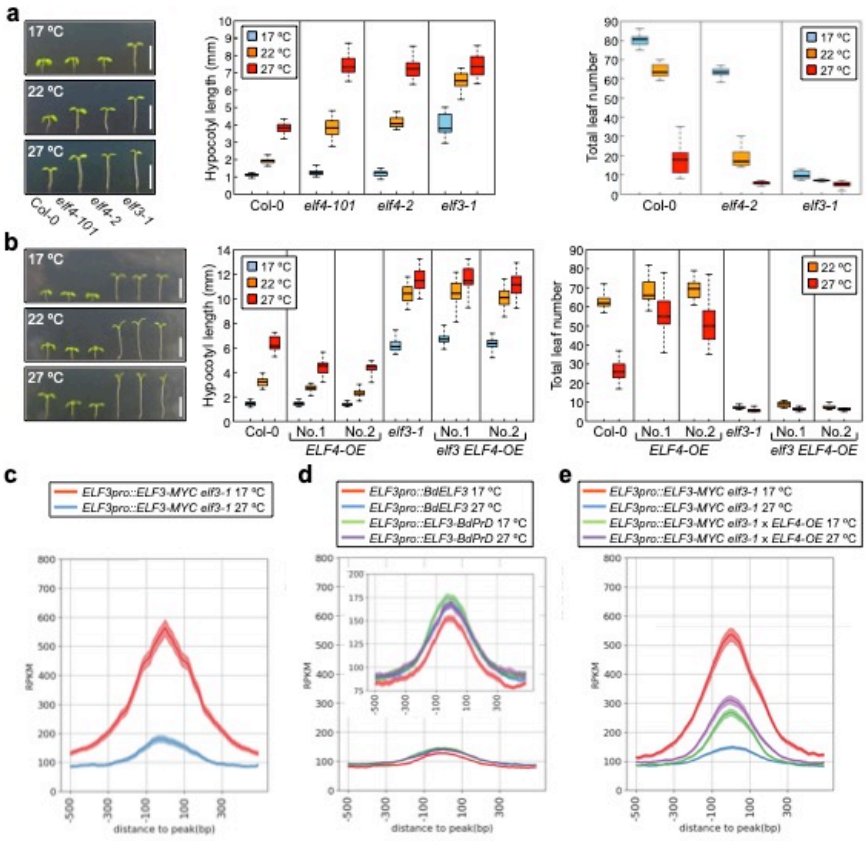

Fig. 2: *ELF4* is required to stabilize the activity of the EC at warmer temperatures.

a, At lower temperatures, *ELF4* becomes dispensable for controlling both hypocotyl elongation and flowering, but with increasing temperature, *ELF4* assumes a greater role. **b**, *ELF4* overexpression greatly reduces thermal responsiveness of both hypocotyl elongation and flowering time, and this response is entirely dependent on *ELF3*. **c**, ELF3 binding at targets, which is measured by ChIP-seq, is temperature dependent and declines genome-wide at 27 ºC. **d**, Transgenic plants with stabilized forms of ELF3 do not respond to temperature. **e**, *ELF4* overexpression stabilizes ELF3 and removes its temperature responsiveness of binding to targets. Scale bars, 5 mm (**a**, **b**)

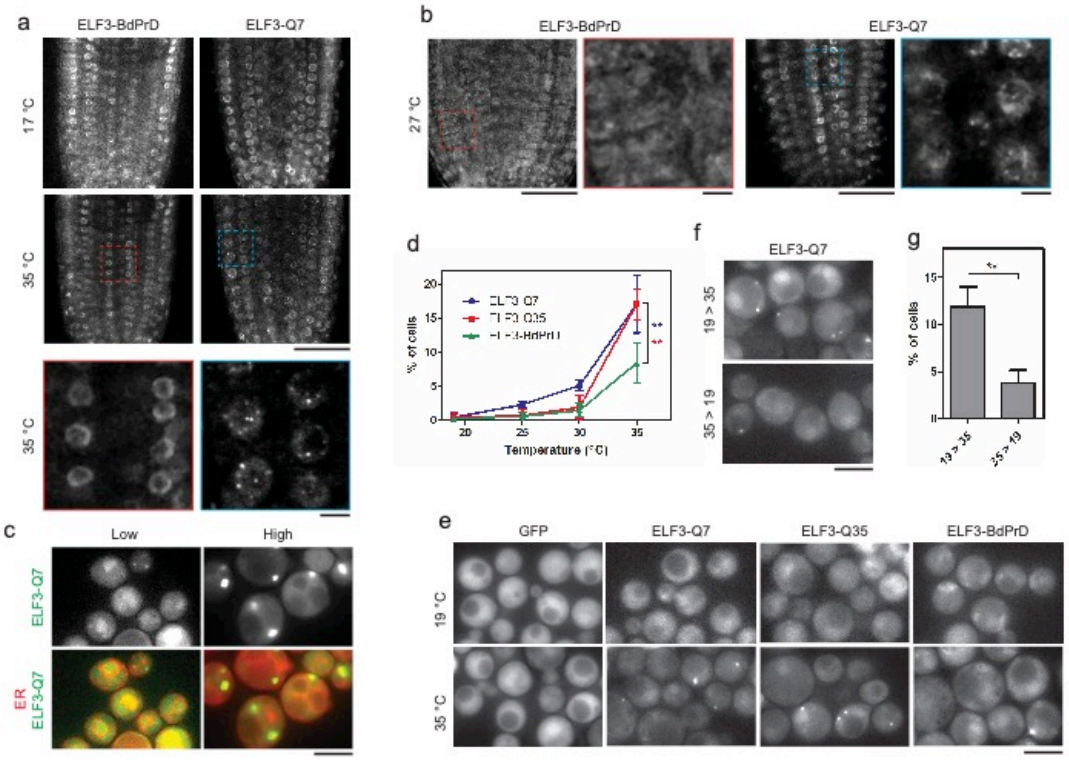

Fig. 3: High temperature induces the formation of ELF3 speckles *in vivo*.
a, Seedlings expressing GFP-tagged ELF3 (Q7) or a chimeric ELF3 where the PrD has been replaced by the corresponding region of *Brachypodium* ELF3 (BdPrD) grown in short photoperiods for 7 days at 17 ºC. Roots imaged by confocal microscopy before and after incubation at 35 ºC for 15 min. **b**, Seedlings as in **a** but shifted to 27 ºC for 2 hours. **c**, *S. cerevisiae* cells expressing GFP-tagged ELF3 (Q7) from a centromeric plasmid (Low) or an episomal plasmid (High), to achieve low or high expression levels of the protein, were grown in selective synthetic complete medium at 30 ºC. Sec63-mCherry was used as an ER reporter. **d**, Quantification of ELF3 speckles in *S. cerevisiae* cells expressing free GFP (GFP only), ELF3 (Q7), ELF3 with a longer polyQ repeat (Q35), or ELF3 with the PrD of *Brachypodium* (BdPrD) were grown overnight at 19 ºC and incubated at the indicated temperatures for 30 min. **e**, Representative images of cells from **d** at 35 ºC. **f**, *S. cerevisiae* cells expressing ELF3 were grown at 19 ºC overnight and incubated at 35 ºC for 30 min (19 > 35) followed by the incubation at 19 ºC for 60 min (35 > 19). Cells shifted from 35 to 19 ºC show a loss of speckles. **g**, Quantification of ELF3 speckles for cells in **f.** Scale bars, 40 µm (**a and b**) and 5 µm (**a and b** inset, **c**, **e, and f**) , ** $p < 0.01$.

.

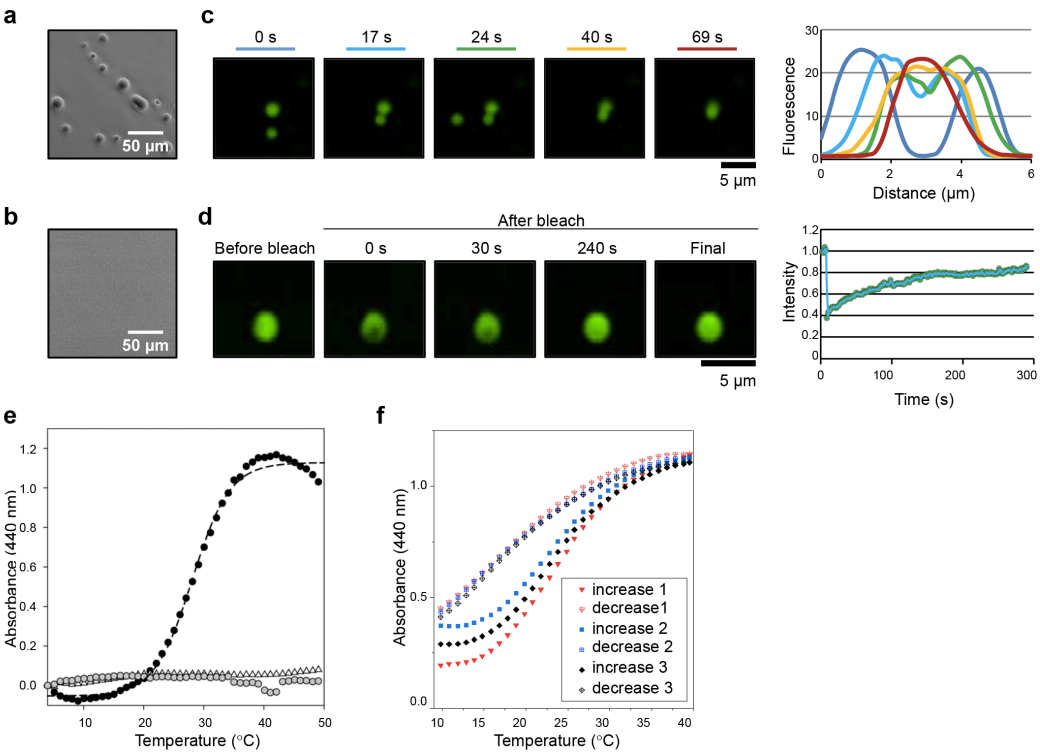

Fig. 4: The PrD of ELF3 undergoes a reversible phase transition in response to temperature.
a, Purified ELF3 PrD peptide forms liquid droplets at 27 ºC *in vitro*. **b**, The equivalent protein domain from BdELF3, which is not predicted to contain a PrD, remains soluble and does not show any liquid droplet formation **c,** Purified ELF3 PrD-GFP protein forms spherical droplets *in vitro*, which fuse. **d,** ELF3 PrD-GFP droplets show rapid recovery after photobleaching, indicating they are liquid droplets. **e**, Light scattering assay as a function of temperature for ELF3 PrD (15 µM; black circle), BdELF3 (15 µM; grey circle) and buffer alone (50 mM CAPS pH 9.7, 150 mM NaCl, 1 mM TCEP; open triangles). Dashed line shows curve-fitting using a 4-parameter sigmoidal equation. The T_m for ELF3 PrD is 28.7 ± 1.8 ºC and the spectrum is representative of three independent experiments. **f**, Reversibility of light scattering as a function of temperature for ELF3 PrD (15 µM; 50 mM CAPS pH 9.7, 200 mM NaCl, 1 mM TCEP). On the same sample, the temperature was increased and decreased three times in succession (1 °C/min). The observed turbidity was reversible and consistently returned to Abs_{440nm} = 0.432 ± 0.02. Interestingly, the initial absorbance reading for repeat 3 (Abs_{440nm} = 0.288) is lower than for repeat 2 (Abs_{440nm} = 0.373) and this is likely due time dependent equilibration (as noted in Extended Figure 12c). The spectra are representative of two independent experiments and similar results were observed for samples at 5 µM. Scale bars, 50 µm (**a**, **b**) and 5 µm (**c**, **d**).